Electrochemical and Solid-State Letters, **14** (7) H303-H305 (2011)
1099-0062/2011/14(7)/H303/3/$28.00 © The Electrochemical Society

Post-Humid Annealing of Low-Temperature Solution-Processed Indium Based Metal Oxide TFTs

Young Hwan Hwang, Jun-Hyuck Jeon, and Byeong-Soo Bae[z]

Laboratory of Optical Materials and Coating (LOMC), Department of Materials Science and Engineering, Korea Advanced Institute of Science and Technology (KAIST), Daejeon 305-701, Korea

Thin-film transistors (TFTs) with indium based metal oxide, aluminum indium oxide, channel layers were fabricated via a simple and low-cost solution process. The process temperature was reduced to 250°C, an applicable temperature to plastic substrates, by applying post-annealing. Post-annealing under various atmospheric conditions effectively converts the remaining In(OH) species to a metal oxide at low temperature. It was revealed that humid O_2 post-annealing mostly facilitated the conversion of In(OH) species to a metal oxide. The optimized low temperature (i.e., 250°C) solution processed AIO TFT exhibits a channel mobility of 2.37 $cm^2/V \cdot s$, a sub-threshold slope of 0.6 V/decade, and an on-to-off current ratio greater than 10^6.
 [DOI: 10.1149/1.3589252]

Manuscript submitted March 23, 2011; revised manuscript received April 15, 2011. Published May 5, 2011.

Increasing demand for large area, high-performance electronics in the last decade has led to the development of a new class of electronic materials—oxide semiconductors.[1,2] Oxide semiconductors offer numerous advantages including transparency originating from their large band gap, high uniformity over large area due to their amorphous nature, environmental stability, and high mobility compared to conventional amorphous silicon and organic semiconductor materials.[3] They are conventionally fabricated via vacuum processes such as atomic layer deposition, ion-beam assisted deposition, pulsed layer deposition, and RF-magnetron sputtering. Various types of oxide semiconductors have been reported since crystalline ZnO and IGZO were introduced: ZnO, In_2O_3, IZO, IGZO, HIZO, and IZTO.[3–5] The vacuum processed oxide semiconductors exhibit good electrical properties and can be prepared at low temperature, and even at room temperature.[6] However, the processes require expensive equipment (incurring high fabrication cost) and the size of the substrate is limited due to the physical restrictions of the chamber.

Solution-processed oxide semiconductors offer additional benefits over vacuum assisted techniques including simplicity, large area uniformity, high throughput, and low fabrication cost. Additionally, the underlying layer, usually a gate dielectric in a thin-film transistor (TFT), is rarely damaged, because the solution process does not involve a harsh environment such as plasma or a high vacuum state. Control of the interface is also an important issue for TFT applications in terms of device stability, since an electron path is created at the interface between the semiconductor and gate dielectric in the bottom-gate type TFT structure.[3]

The fabrication process of the oxide film in this method is simple, entailing coating of the precursor solution and annealing. This process offers the formation of diverse oxide semiconductor materials from single metal oxides to multi composite oxides: ZnO, IZO, ZTO, IGZO, and AIO.[7–12] During the process, the metal precursor undergoes thermal decomposition and oxidation reaction. The precursor based method requires high annealing temperature, usually over 400°C, to enhance or promote the oxidation reaction and remove the unnecessary carbon groups. These groups usually deteriorate the electrical properties and give rise to negative phenomena, such as electron capturing and hindering of electron movement.[7]

Various approaches have been suggested in efforts to realize a low temperature process. It was reported that controlled hydrolysis and a condensation reaction on a chip in an inert nitrogen atmosphere can reduce the annealing temperature to 230°C.[13] However, the use of unique precursors that are sensitive to the ambient gases (i.e., H_2O and O_2), and fabrication under a closed atmosphere restrict application of the process. Previously, we have applied vacuum post-annealing to a zinc tin oxide TFT to accomplish high performance with low annealing temperature by forming oxygen vacancies and removing impurity ions.[14]

[z] E-mail: bsbae@kaist.ac.kr

In this study, we report on the effects of post-annealing, which is employed to decrease the process temperature, on indium based metal oxide TFTs. Post-annealing was applied under ambient air, humid air, and a humid oxygen atmosphere, respectively, to investigate the consequences of water molecules and the oxidation power of the gas during the annealing process. The compositions of the post-annealed films, analyzed by X-ray photoelectron spectroscopy (XPS), and their electrical properties were studied.

The synthesis of the precursor solution starts with dissolving 0.1 M of indium acetylacetonate [$In(C_5H_7O_2)_3$, Aldrich] and 0.04 M of aluminum acetylacetonate [$Al(C_5H_7O_2)_3$, Aldrich] in 2-methoxyethanol [$C_3H_8O_2$, Alrich]. In this report, we employed indium acetylacetonate, which is decomposed at low temperature, rather than indium acetate as an indium source, used in a previous report.[11] Since the solubility of indium acetate is very limited, an additional stabilizer, which could increase the decomposition temperature, is required to obtain a stable, transparent, and homogeneous precursor solution. The precursor solution was stirred at 50°C for 24 h to make a transparent and homogeneous solution. After sufficient reaction, the solution was filtered through a 0.22 μm syringe filter (PTFE, GE) and spin-coated at a speed of 5000 rpm atop of the SiO_2/Si substrate for 30 s. A 100 nm SiO_2 layer, which served as a gate dielectric, was thermally grown on top of the heavily boron (p+) doped silicon wafer. After film deposition, the film was annealed on a hot plate at given temperature under ambient air. A bottom-gate, top-contact type structure was used for characterizing the fabricated TFTs. 100 nm aluminum source and drain electrodes were deposited by an e-beam evaporator through a shadow mask under pressure of $\sim 10^{-6}$ Torr. The fabricated channel length and width were 100 and 1000 μm, respectively. After the fabrication of TFTs, the performances of the devices were measured in a dark room under the ambient atmosphere using a HP 4155A semiconductor parameter analyzer.

The results of the thermogravimetric analysis (TGA), shown in Fig. 1, indicate that thermal decomposition of the precursor solution is completed at around 310°C. The abrupt weight loss between 150 and 200°C is attributed to thermal decomposition of organic anion groups and evaporation of the residual solvent. The slight weight loss shown at ~300°C is ascribed to the conversion of In(OH) to a metal oxide. According to the TGA, it is reasonable to conclude that the appropriate annealing temperature is over 310°C, which is still a high temperature for flexible electronics. Another notable aspect with TGA is that only the conversion reaction is preceded for oxide formation after 250°C.[15] This suggests that there is sufficient room for decreasing the process temperature by promoting the conversion reaction.

The transfer characteristics of I_D versus V_G at $V_{DS} = 40$ V, displayed in Fig. 2a, show significant change of the electrical properties by annealing temperature. The AIO TFT annealed at 350°C shows good electrical performance while the 250°C annealed TFT

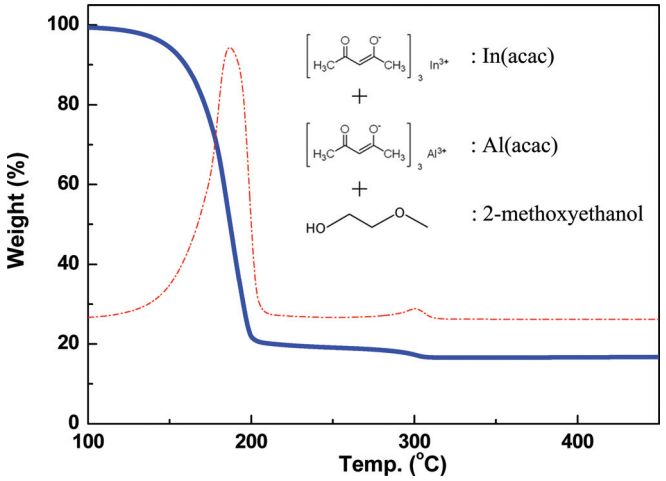

Figure 1. (Color online) Thermogravimetric analysis of AIO precursor solution, containing In(acac) and Al(acac) in 2-methoxyethanol.

does not. The electrical parameters including the saturation mobility and the threshold voltage were derived from a linear fitting to the plot of the square root of I_D versus V_G using the following equation in the saturation region

$$I_D = \frac{WC_i}{2L}\mu(V_G - V_{th})^2$$

Here, W, L, μ, C_i, and V_{th} are the channel width, channel length, channel mobility, capacitance per unit area of the SiO_2 gate insulator (dielectric constant ~3.9), and threshold voltage, respectively. The AIO TFT annealed at 350°C, which provides sufficient thermal energy for complete thermal decomposition, exhibits much higher mobility of 13.4 $cm^2/V{\cdot}s$ and an on-to-off current ratio of 10^8 while the 250°C annealed TFT shows values of 0.36 $cm^2/V{\cdot}s$ and 10^6; the calculated electrical parameters are listed in Table I.

In solution processed oxide TFTs, higher temperature processed devices usually exhibit better electrical properties.[7,11] It is understood that the advanced performance with higher temperature annealing is attributed to improved local atomic rearrangement, modification of the semiconductor/dielectric interface, or a decrease in the gap state and/or the tail state near the conduction band minimum at high temperature.[16] However, high annealing temperature, which is the most simple and efficient way to improve the electrical properties of the device, restricts the use of various substrates such as soda-lime glass or flexible plastic substrates.

The XPS analysis of 350 and 250°C annealed AIO thin films, shown in Fig. 2b, indicates that the insufficient electrical properties of the 250°C annealed AIO TFT can be attributed to a large amount of remaining In(OH) species. A clear indium oxide peak, shown at 529.9 eV, appears in both cases.[17] However, a large amount of In(OH) species, found at 532 eV, is observed in the 250°C annealed thin film. In contrast, the 350°C annealed film, which exhibits good electrical properties in terms of on-current and mobility, has very little In(OH) species.[10,13] The XPS analysis results, which are identical to the TGA of the precursor solution, imply that annealing at 250°C does not offer sufficient thermal energy to form oxides of the metal species. Since a large amount of In(OH) species, which is

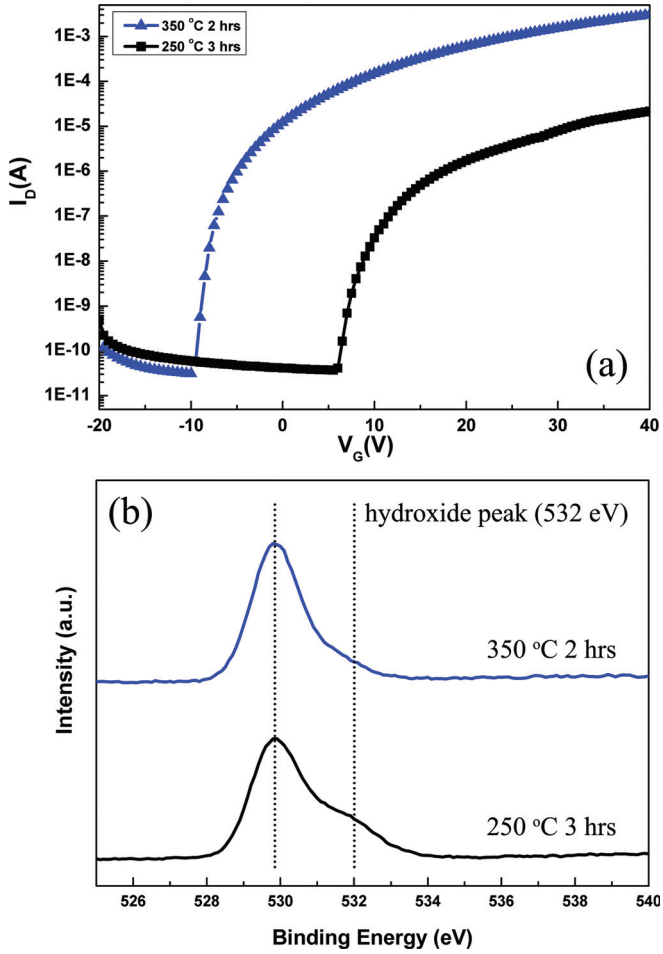

Figure 2. (Color online) (a) Transfer characteristics of AIO TFTs and (b) O 1s core level XPS for AIO thin films, annealed at 250 and 350°C. The dashed lines indicate the peaks originating from oxide lattices without oxygen vacancies (~529.9 eV) and hydroxide (~532 eV), respectively.

detected in very slight quantities in the case of the AIO TFT annealed at 350°C, remains inside the film, the electrical properties of the film are restricted, as can be anticipated.

In order to improve the performance of the device with a low temperature process by promoting the conversion of In(OH) to a metal oxide, post-annealing was applied. The AIO thin films were prepared by spin coating and annealing at 250°C for 2 h. After film deposition, the samples were additionally annealed at 250°C for 1 h under various atmospheres: ambient air, humid air, and humid O_2, respectively. The humidity was fixed to ~85% by controlling the pressure and flow of the carrier gas.

The effects of post-annealing on the composition of the AIO thin films were investigated by XPS, and the results are displayed in Fig. 3a. The peak of In(OH) species in the AIO thin films was clearly reduced by humid post-annealing. The amount of the decline was greater with the higher oxidation power gas, that is, humid O_2. The results imply that unnecessary In(OH) species, in terms of electrical performance, are effectively converted to a metal oxide by humid

Table I. Calculated electrical parameters of the AIO TFTs with different annealing conditions.

Temperature (°C)	Ambient-annealing (h)	Post-annealing (h)	Mobility ($cm^2V^{-1}s^{-1}$)	Ion/Ioff	S.S. (V/decade)
350	2	N.A.	13.4	9.8×10^7	0.5
250	2	1 (ambient air)	0.36	6.0×10^6	0.7
250	2	1 (humid air)	1.31	3.1×10^6	0.6
250	2	1 (humid O_2)	2.37	6.5×10^6	0.6

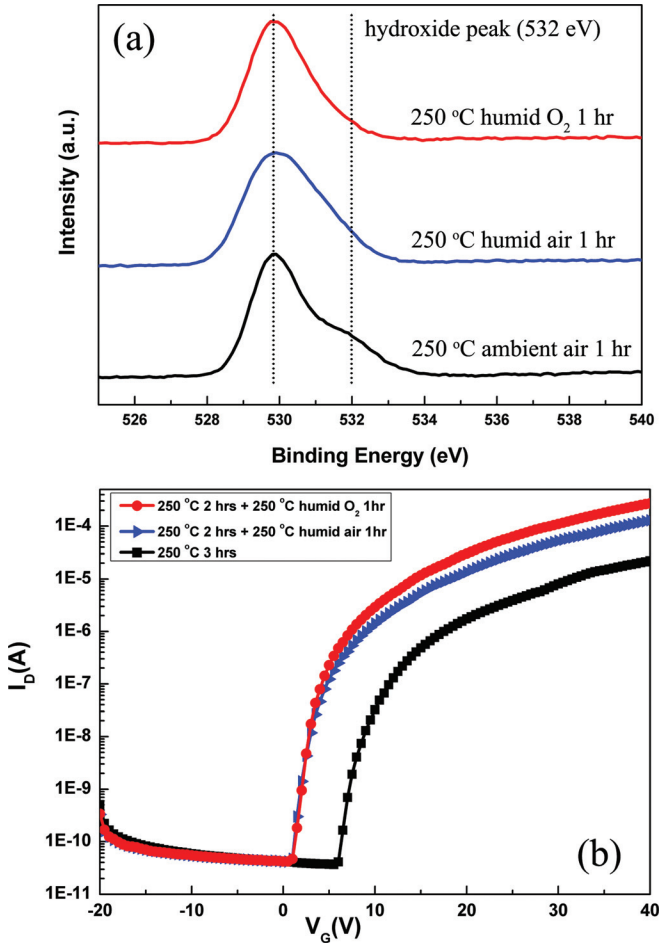

Figure 3. (Color online) (a) O 1s core level XPS spectra for AIO thin films and (b) transfer characteristics of AIO TFTs, post-annealed with ambient air, humid air, and humid O_2 at 250°C. The dashed lines indicate the peaks originating from oxide lattices without oxygen vacancies (~529.9 eV) and hydroxide (~532 eV), respectively.

post-annealing. It was also observed that the amounts of In(OH) species, which are estimated by a XPS analysis in Figs. 2b and 3a, in the 350°C annealed film and the humid O_2 post-annealed film at 250°C were similar.

The compositional evolution of the humid annealed AIO thin film implies that water molecules play a decisive role during the oxide formation process. The XPS analysis indicates that the formation of the metal oxide is facilitated by water molecules under the same thermal energy. In addition, higher conversion with humid O_2 post-annealing implies that the oxidation power of the atmosphere gas during the annealing process also affects the formation of the oxide. Thus, it seems reasonable to conclude that the activation energy to convert In(OH) to the metal oxide is lowered by water molecules existing in the atmosphere gas, and the reaction is also accelerated by higher oxidation power gas.

The transfer curves, presented in Fig. 3b, show the enhancement of electrical performance by post-annealing. It was observed that the on-current of the devices was increased by more than a factor of 10, the sub-threshold slope was slightly improved, and the transfer curves tended to shift to negative voltage by post-annealing under humid gas; the calculated electrical parameters are listed in Table I. In particular, the mobility was increased to 1.31 and 2.37 $cm^2/V{\cdot}s$ with humid air and humid O_2 post-annealing, respectively. Since hydrogen-containing molecules often cause deterioration of electrical performance and the stability of the device, it appears that the improved electrical properties of the post-annealed devices can be attributed to facilitated conversion of In(OH) to the metal oxide.[18,19]

In conclusion, we have applied post-annealing to improve the electrical properties of solution processed AIO TFTs fabricated at 250°C. The post-annealing was applied under ambient air, humid air, and a humid O_2 atmosphere, respectively. The In(OH) species, observed in minute quantities in the 350°C processed AIO TFTs, were effectively converted to a metal oxide by humid post-annealing, while a large amount of In(OH) species remained with ambient post-annealing. The electrical properties of the device were improved as a consequence of humid O_2 annealing, which facilitates conversion of In(OH) to the metal oxide. The results reveal that post-annealing under higher oxidation power gas and humidity is an effective tool to enhance the performance of TFT devices.

Acknowledgment

This research is financially supported by the Ministry of Knowledge Economy (MKE) and Korea Institute for Advancement in Technology (KIAT) through the Workforce Development Program in Strategic Technology. This research was supported by Basic Science Research Program through the National Research Foundation of Korea (NRF) funded by the Ministry of Education, Science and Technology (CAFDC-20100009898).

References

1. J. F. Wager, *Science*, **300**, 1245 (2003).
2. K. Nomura, H. Ohta, A. Takagi, T. Kamiya, M. Hirano, and H. Hosono, *Nature (London)* **432**, 488 (2004).
3. T. Kamiya, K. Nomura, and H. Hosono, *Sci. Technol. Adv. Mater.*, **11**, 044305 (2010).
4. C. J. Kim, S. W. Kim, J. H. Lee, J. S. Park, S. I. Kim, J. C. Park, E. H. Lee, J. C. Lee, Y. S. Park, J. H. Kim, et al., *Appl. Phys. Lett.*, **95**, 252103 (2009).
5. D.-H. Cho, S. Yang, C. Byun, J. Shin, M. K. Ryu, S.-H. Ko Park, C.-S. Hwang, S. M. Chung, W.-S. Cheong, S. M. Yoon, et al., *Appl. Phys. Lett.*, **93**, 142111 (2008).
6. E. M. C. Fortunato, P. M. C. Barquinha, A. C. M. B. G. Pimentel, A. M. F. Goncalves, A. J. S. Marques, L. M. N. Pereira, and R. F. P. Martins, *Adv. Mater.*, **17**, 590 (2005).
7. Y. H. Hwang, S.-J. Seo, and B.-S. Bas, *J. Mater. Res.*, **25**, 695 (2010).
8. C. G. Choi, S.-J. Seo, and B.-S. Bae, *Electrochem. Solid-State Lett.*, **11**, H7 (2008).
9. S.-J. Seo, C. G. Choi, Y. H. Hwang, and B.-S. Bae, *J. Phys. D: Appl. Phys.*, **42**, 035106 (2009).
10. S. Jeong, Y.-G. Ha, J. Moon, A. Facchetti, and T. J. Marks, *Adv. Mater.*, **22**, 1346 (2010).
11. Y. H. Hwang, J. H. Jeon, S.-J. Seo, and B.-S. Bae, *Electrochem. Solid-State Lett.*, **12**, H336 (2009).
12. B. Sun and H. Sirringhaus, *Nano Lett.*, **5**, 2409 (2005).
13. K. K. Banger, Y. Yamashita, K. Mori, R. L. Peterson, T. Leedham, J. Rickard, and H. Sirringhaus, *Nature Mater.*, **10**, 45 (2011).
14. S.-J. Seo, Y. H. Hwang, and B.-S. Bae, *Electrochem. Solid-State Lett.*, **13**, H357 (2010).
15. T. Sato, *J. Therm. Anal. Calorim.*, **82**, 1388 (2005).
16. H. Q. Chiang, R. L. Hoffman, J. Jeong, D. A. Keszler, and J. F. Wager, *Appl. Phys. Lett.*, **86**, 013503 (2005).
17. D.-H. Lee, S.-Y. Han, G. S. Herman, and C.-H. Chang, *J. Mater. Chem.*, **19**, 3135 (2009).
18. K. Nomura, T. Kamiya, H. Ohta, M. Hirano, and H. Hosono, *Appl. Phys. Lett.*, **93**, 192107 (2008).
19. K. Nomura, T. Kamiya, M. Hirano, and H. Hosono, *Appl. Phys. Lett.*, **95**, 013502 (2009).